Supplemental Information for

CHIP regulates Aquaporin-2 Quality Control and Body Water Homeostasis

Table of Contents

Supplemental Table 7. Detailed information on Antibodies

Antibody	Supplier	Cat. No. or Reference	Predicted MW (kDa)
Ubiquitin	Cell Signaling	3936	N/A
PSMD14	Cell Signaling	4197	35
USP14	Cell Signaling	11931	60
USP4	Cell Signaling	2651	110
OTUB1	Abcam	ab82154	31
RNF128	Abcam	ab72533	45-70
CHIP (Stub1)	Abcam	ab134064	35
Proteasome 20S	Abcam	ab3325	30
AQP3	Abcam	ab153694	25 and 32-40
CSN6	Santa Cruz	sc47965	34
USP5	Santa Cruz	sc366624	96
USP7	Santa Cruz	sc30164	135
USP32	Santa Cruz	sc374465	130-190
USP47	Santa Cruz	sc100633	157
FBXO2	Santa Cruz	sc393873	42
FBXO29	Santa Cruz	sc514385	60-70
Ure-b1	Santa Cruz	sc49768	400
Six4	Santa Cruz	sc55766	80
Smad4	Santa Cruz	sc7966	60
Nek9	Santa Cruz	sc50765	120
NRK1	Santa Cruz	sc398852	25
HSP70	Enzo	ADI-SPA-810	70
Hsc70	Enzo	ADI-SPA-815	71
ROMK	Novus	NBP1-82874	45
CHIP (Stub1)	Novus	NBP2-47510	35
AQP4	Alamone	AQP-004	30
Actin	Sigma-Aldrich	A2228	42
AQP2 9398	N/A	Moeller HB, Aroankins TS, Slengerik-Hansen J, Pisitkun T, Fenton RA: Phosphorylation and ubiquitylation are opposing processes that regulate endocytosis of the water channel aquaporin-2. *J Cell Sci* 127: 3174-3183, 2014	25 and 35-45
pS256-AQP2	N/A	Hoffert JD, Fenton RA, Moeller HB, Simons B, Tchapyjnikov D, McDill BW, Yu MJ, Pisitkun T, Chen F, Knepper MA: Vasopressin-stimulated increase in phosphorylation at Ser269 potentiates plasma membrane retention of aquaporin-2. *J Biol Chem* 283**:** 24617-24627, 2008	25 and 35-45
NKCC2	N/A	Ecelbarger CA, Terris J, Hoyer JR, Nielsen S, Wade JB, Knepper MA. Localization and regulation of the rat renal Na(+)-K(+)-2Cl- cotransporter, BSC-1. *Am J Physiol* 271: F619–F628, 1996	140
pNKCC2	N/A	Dimke H, et al. Acute growth hormone administration induces antidiuretic and antinatriuretic effects and increases phosphorylation of NKCC2. *Am J Physiol Renal Physiol* 292: F723–F735, 2007	140
NHE3	N/A	Kim GH, Ecelbarger C, Knepper MA, Packer RK. Regulation of thick ascending limb ion transporter abundance in response to altered acid/base intake. *J Am Soc Nephrol* 10: 935–942, 1999	75
NaKATPase (α1 subunit)	N/A	Kashgarian, M., Biemesderfer, D., Caplan, M., and Forbush, B. 3rd.. Monoclonal antibody to Na,K-ATPase: immunocytochemical localization along nephron segments. *Kidney Int* 28: 899–913, 1985	90
Alpha-ENaC	N/A	Sorensen MV, et al. Rapid dephosphorylation of the renal sodium chloride cotransporter in response to oral potassium intake in mice. *Kidney Int* 83: 811–824, 2013	90 and 25 (cleaved)
Gamma-ENaC	N/A	Masilamani S, Kim GH, Mitchell C, Wade JB, Knepper MA. Aldosterone-mediated regulation of ENaC alpha, beta, and gamma subunit proteins in rat kidney. *J Clin Invest* 104:R19–R23, 1999	85

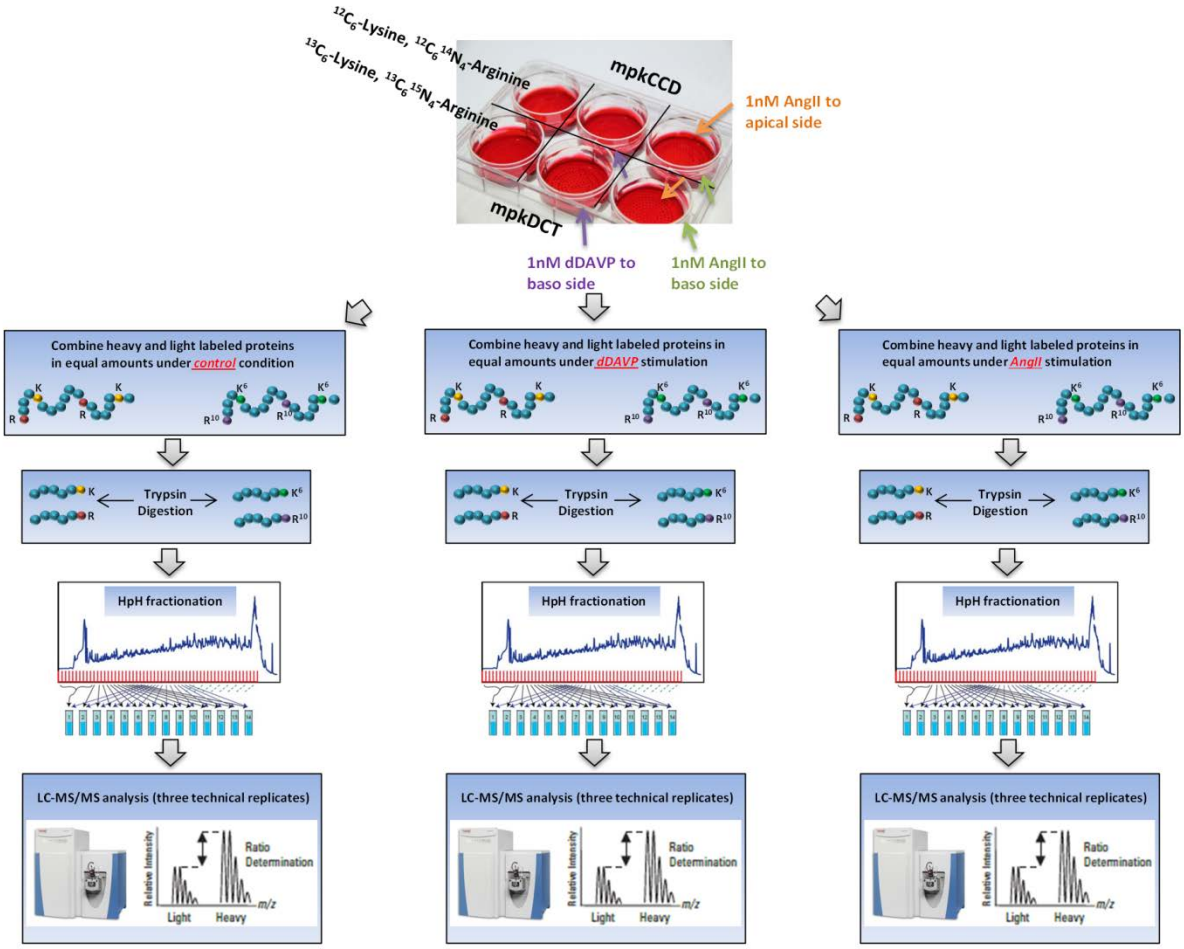

Supplemental Figure 1. Proteomics experimental workflow. mpkDCT cells were cultured in heavy SILAC medium (Lys+6, Arg+10) while mpkCCD cells in light SILAC medium (Lys+0, Arg+0). Four passages of labelled cells were used to generate four biological replicates for statistical analysis. In addition to control conditions, cells were also stimulated for 4 days with the vasopressin type II receptor agonist 1-desamino-8-D-arginine vasopressin (dDAVP, 1nM, only to basolateral (baso) side) or angiotensin-2 (ANGII, 1nM, to both apical and basolateral sides). Cells were harvested, equally pooled and subjected to offline high-pH fractionation based two dimensional LC-MS/MS analysis (Q-Exactive).

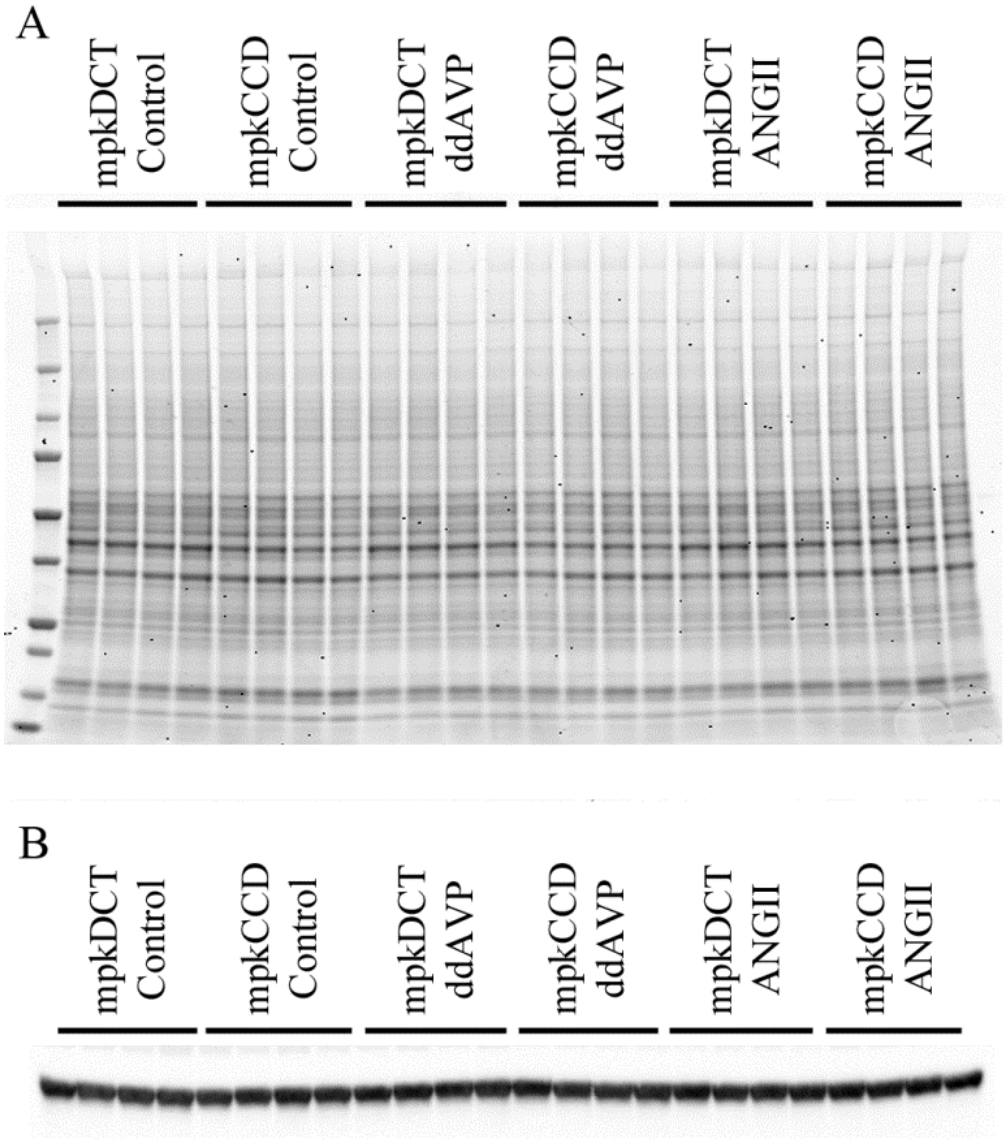

Supplemental Figure 2. Loading controls for immunoblotting of mpkDCT and mpkCCD cells. Equal protein equivalents of samples isolated from the different cell types and different treatments were used for subsequent immunoblotting as demonstrated by Coomassie gel (A) or immunoblot of actin (B).

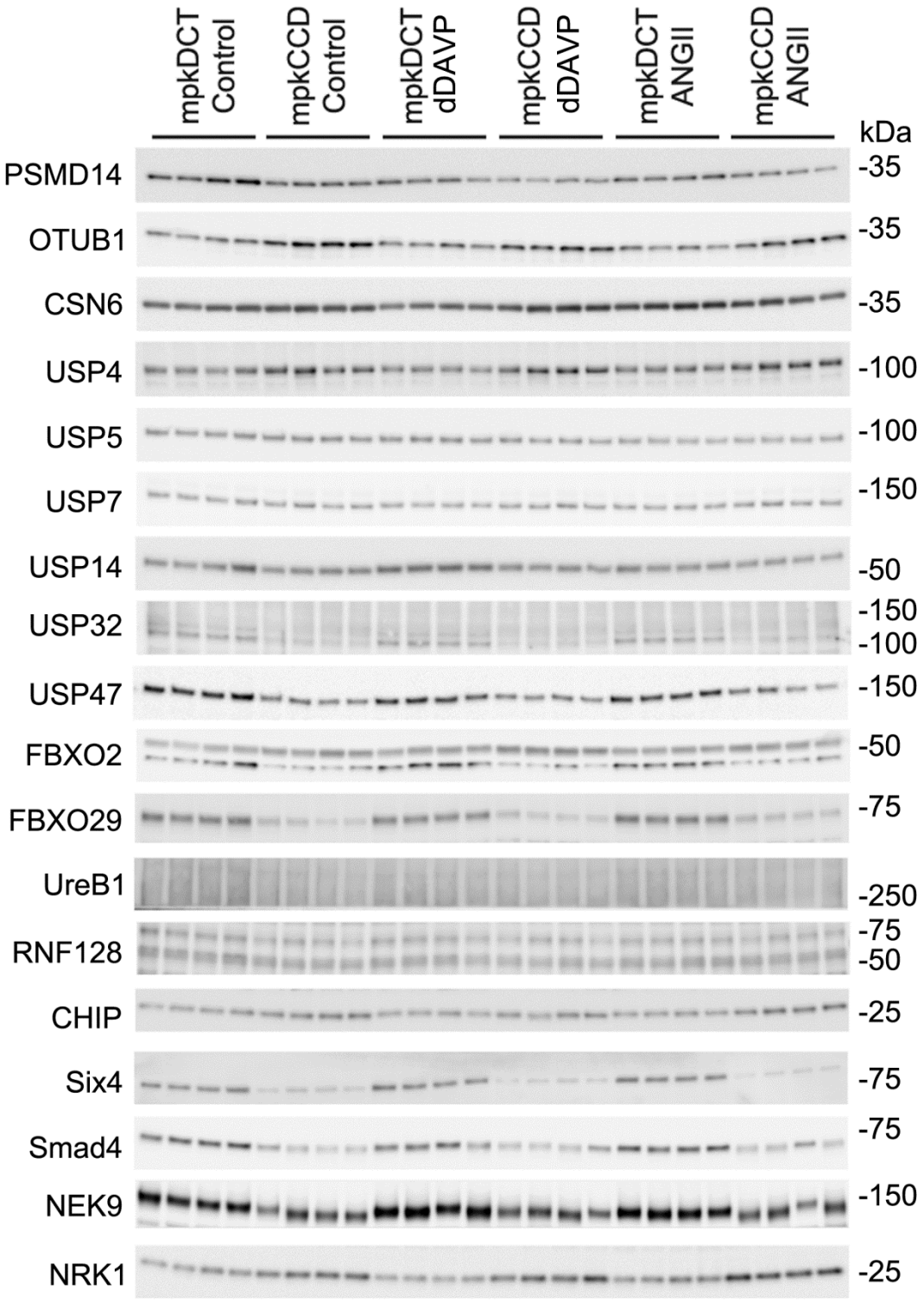

Supplemental Figure 3. Immunoblotting for a variety of the regulatory proteins identified in mpkDCT or mpkCCD cells. Specificity of the commercial antibodies was based on that they either gave a single unique band on an immunoblot corresponding to the target proteins predicted molecular weight, or the most prominent band on the immunoblot was at the target proteins predicted molecular weight (with no other bands of similar size).

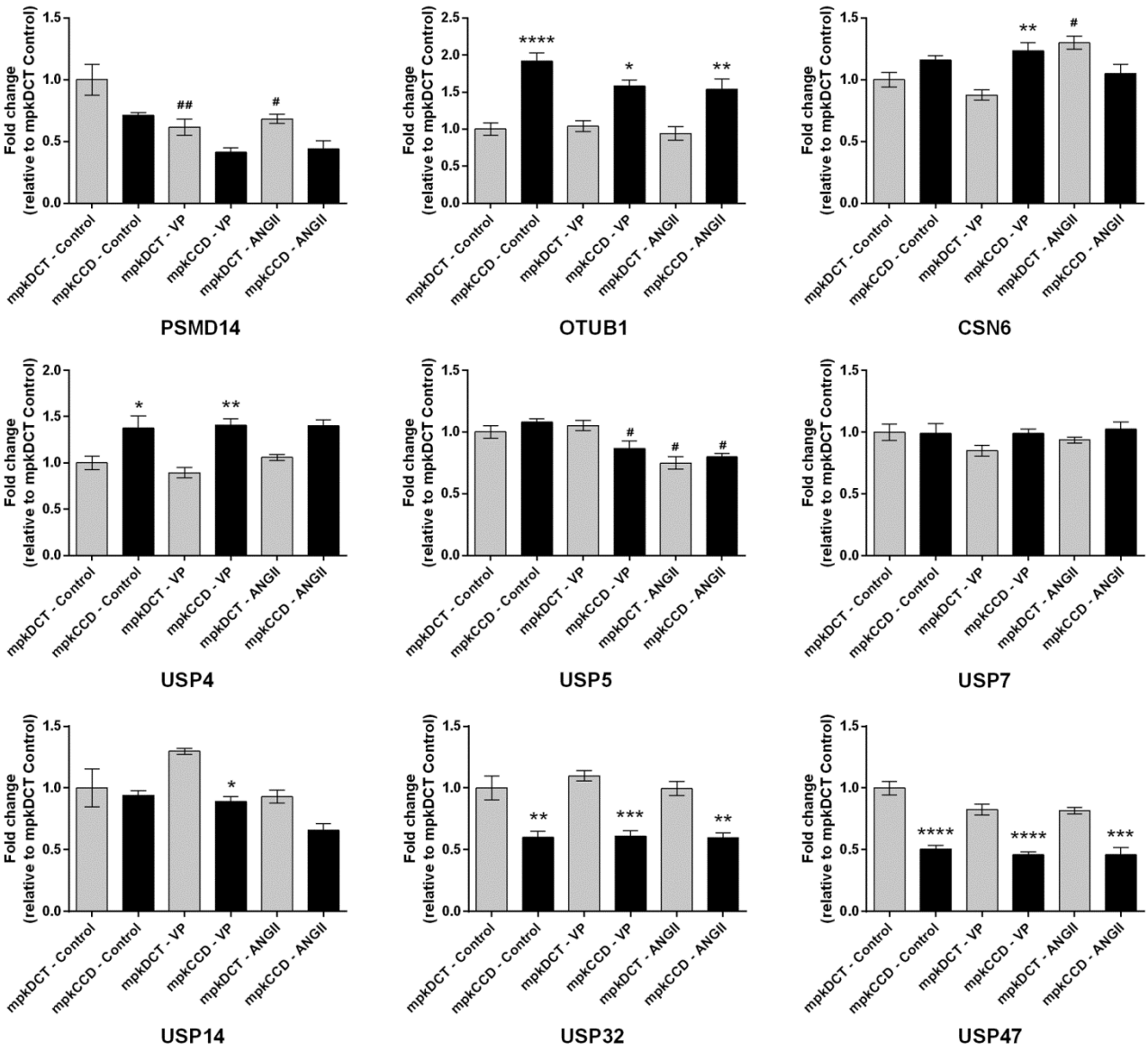

Supplemental Figure 4. Immunoblot quantification of selected DUB genes in mpkDCT and mpkCCD cells grown under three conditions. The mpkDCT control condition was set as baseline, and all other quantifications were relative to mpkDCT control condition. * denotes significance between DCT and CCD under the same condition (DCT used as reference) while # denotes significance within one cell type under different conditions (control condition used as reference). *or #: 0.01<p<0.05; ** or ##: 0.001<p<0.01; *** or ###: 0.0001<p<0.001; **** or ####: p<0.0001.

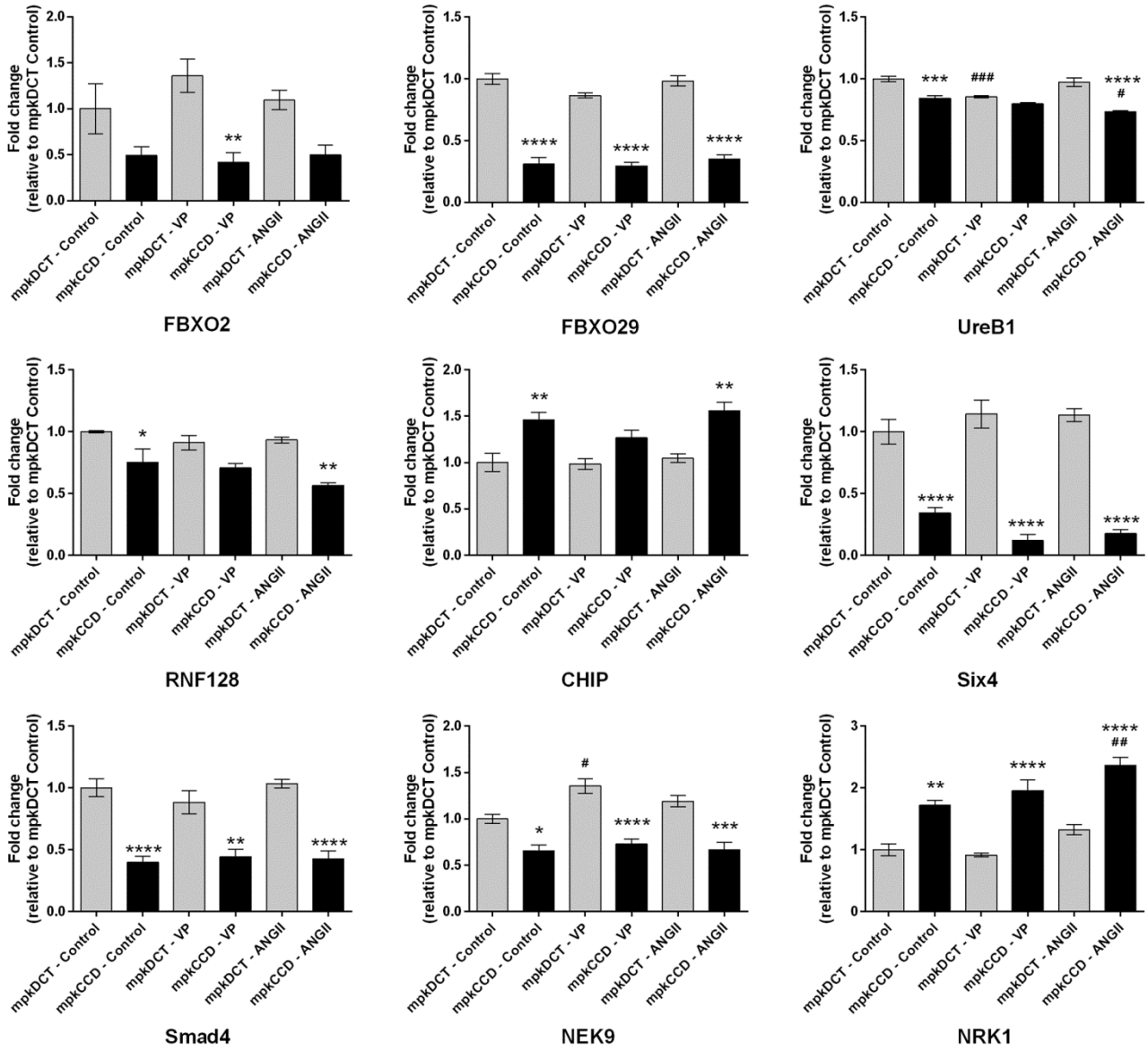

Supplemental Figure 5. Immunoblot quantification of selected kinase, E3 ligase and TF genes in mpkDCT and mpkCCD cells grown under three conditions. The mpkDCT control condition was set as baseline, and all other quantifications were relative to mpkDCT control condition. * denotes significance between DCT and CCD under the same condition (DCT used as reference) while # denotes significance within one cell type under different conditions (control condition used as reference). *or #: 0.01<p<0.05; ** or ##: 0.001<p<0.01; *** or ###: 0.0001<p<0.001; **** or ####: p<0.0001.

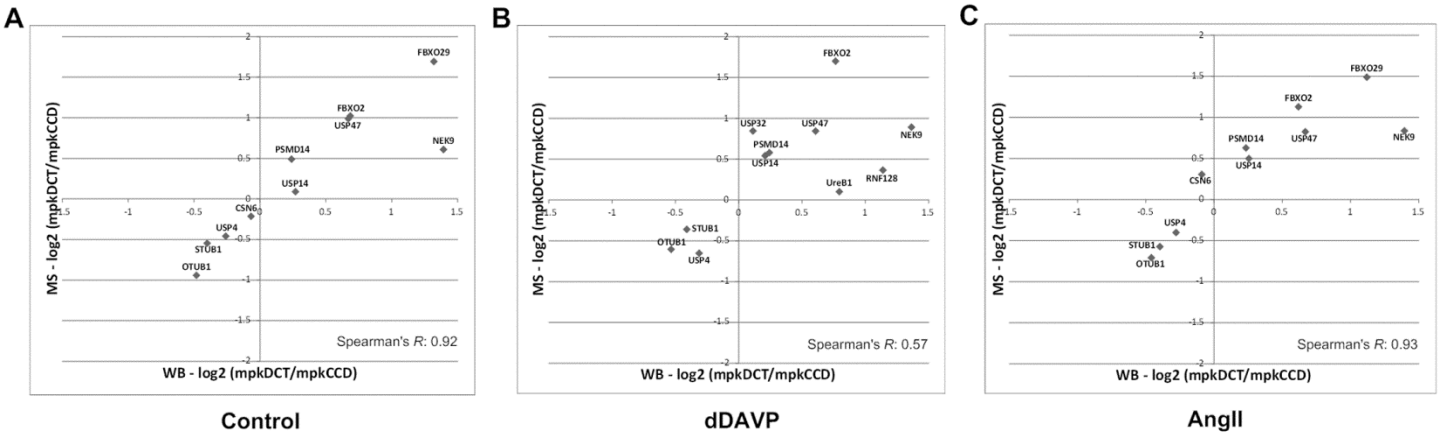

Supplemental Figure 6. The correlation between immunoblot based quantification and mass spectrometry based quantification for selected genes in mpkDCT and mpkCCD cells grown under three conditions. (A) Control condition; (B) dDAVP treatment; (C) AngII treatment. The spearman's correlation coefficient was calculated for each condition.

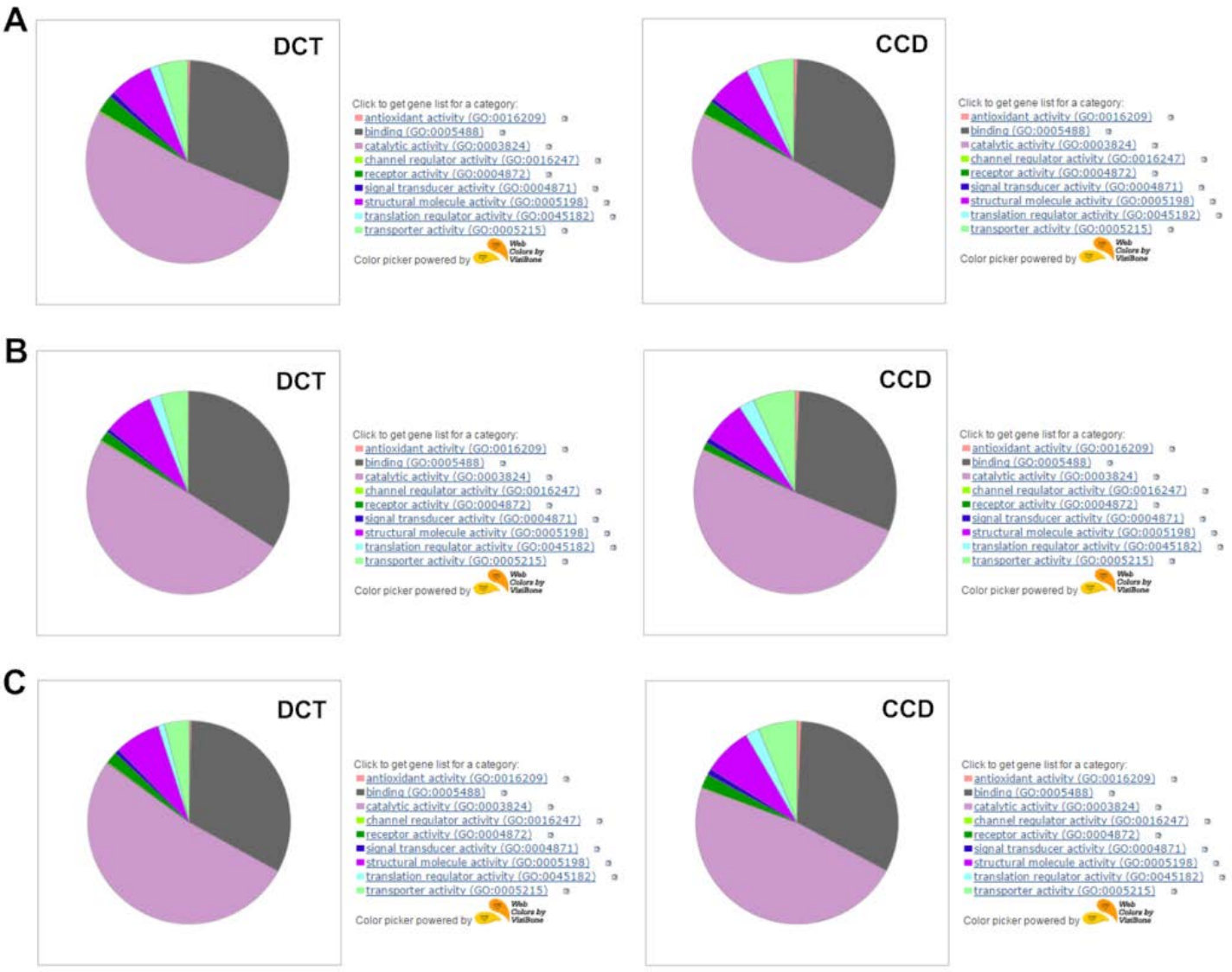

Supplemental Figure 7. GO-term molecular function analysis by Panther. (A) Control condition; (B) dDAVP treatment; (C) AngII treatment. Cell specific genes under each condition were used as Panther inputs.

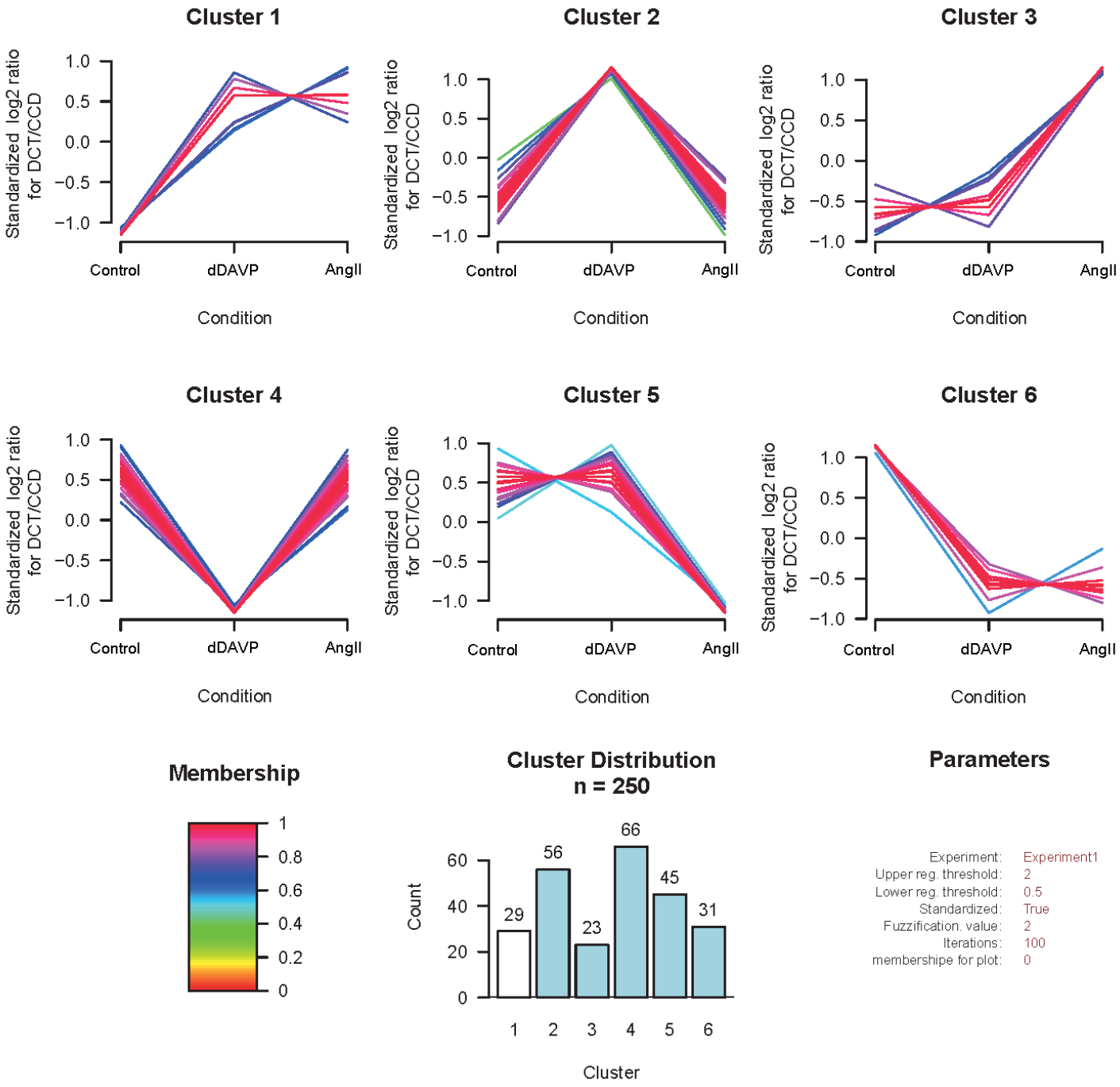

Supplemental Figure 8. Cluster analysis of 250 proteins with the largest standard deviations under three conditions showed 6 distinctive clusters. The data indicates that dDAVP and AngII can have similar – or independent – effects on a subset of proteins in mpkDCT or mpkCCD cells. For example, the abundance of proteins in Clusters 2 and 4 are specifically regulated by dDAVP (but not by AngII), the abundance of proteins in Clusters 3 and 5 are specifically regulated by AngII (but not by dDAVP), whereas the abundance of proteins in Clusters 1 and 6 can be regulated by both dDAVP or AngII.

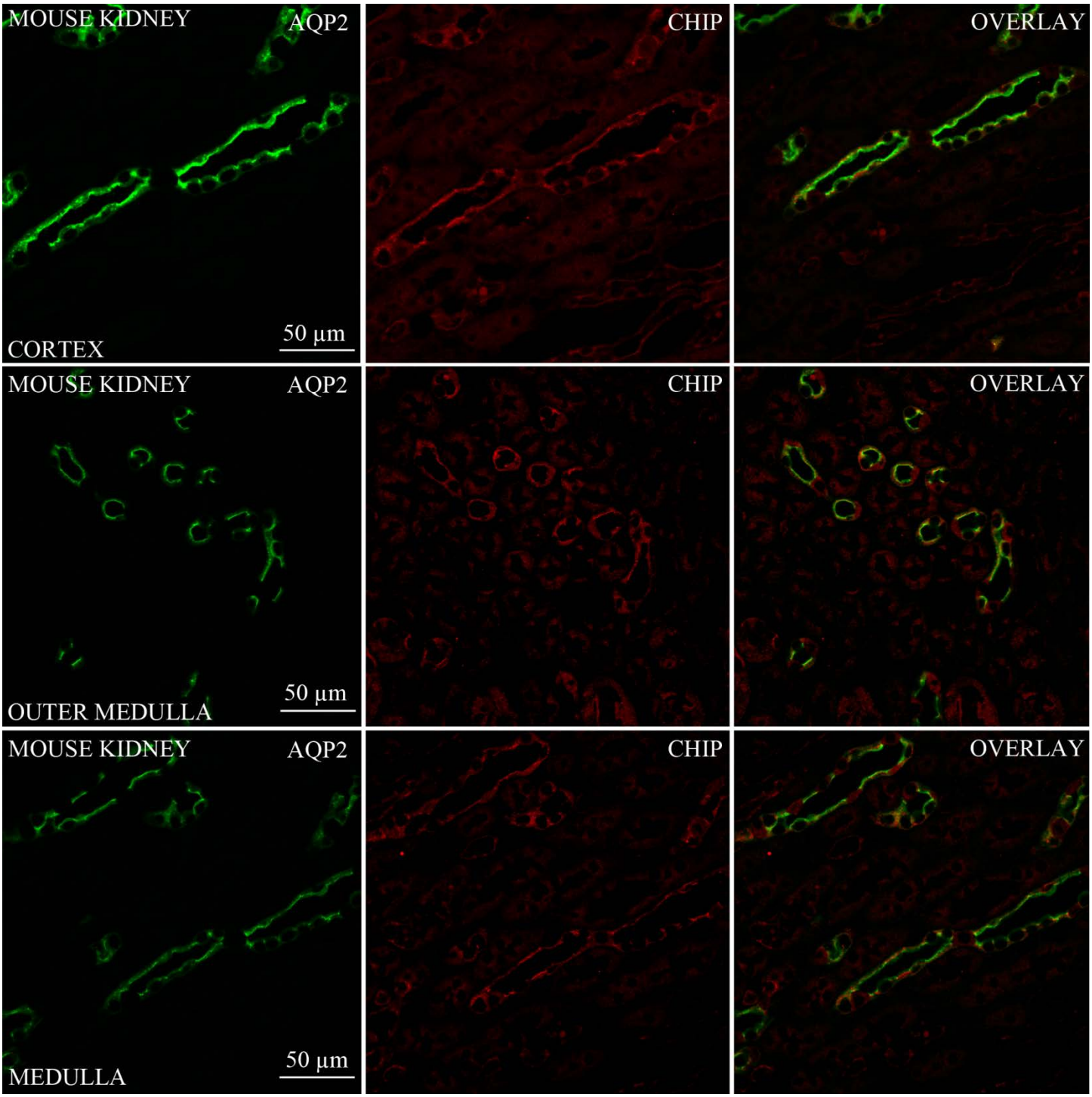

Supplemental Figure 9. Immunohistochemical localization of CHIP in mouse kidney. Confocal images of CHIP and AQP2 distribution in mouse kidney cortex, outer medulla and medulla. CHIP is expressed in principal cells throughout the collecting duct system where it partially colocalizes with AQP2.

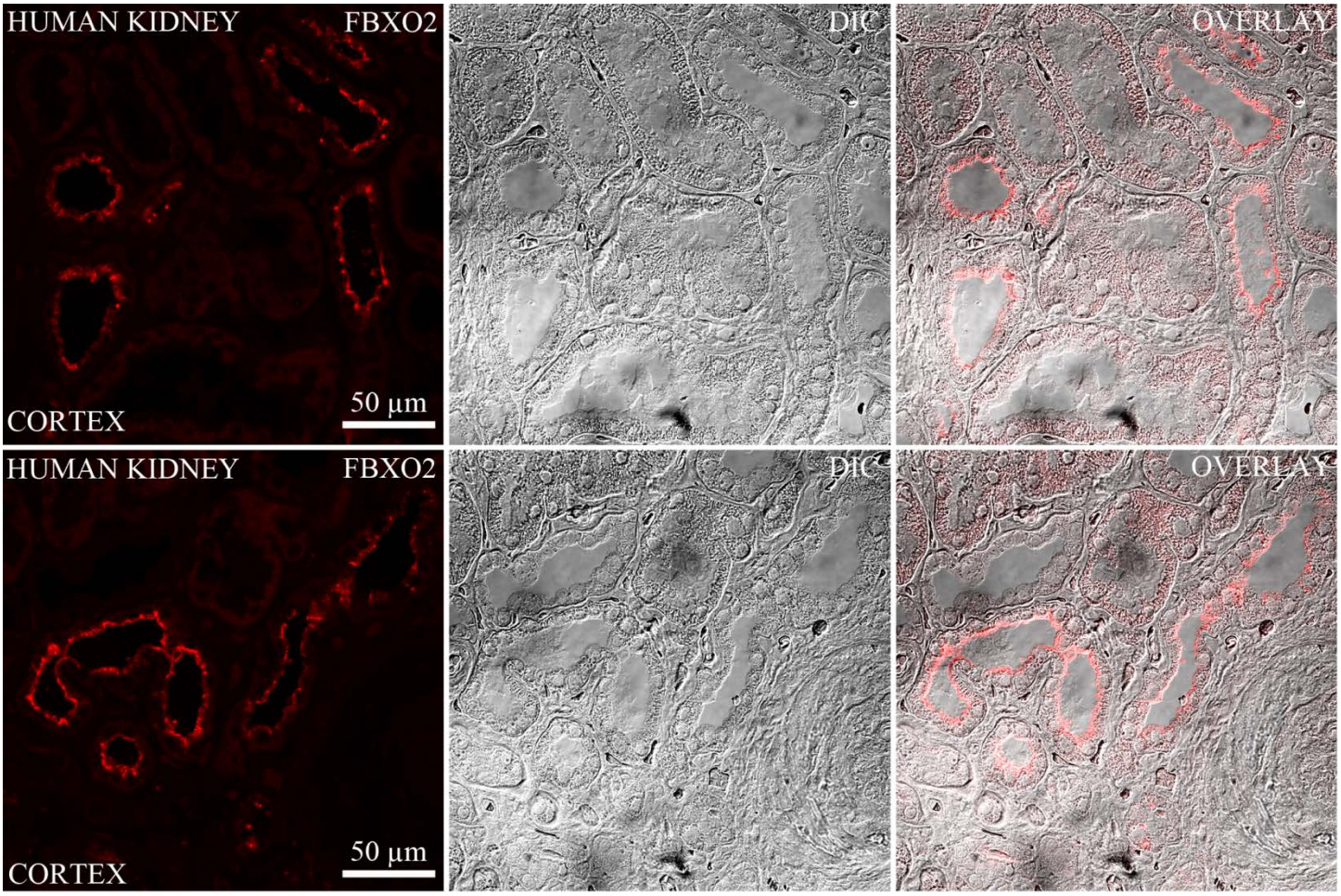

Supplemental Figure 10. Immunohistochemical localization of FBXO2 in human kidney. Confocal images of FBXO2 distribution in human kidney cortex. Differential interference contrast (DIC) images are provided to demonstrate the structure of the imaged section. FBXO2 is localized to tubules morphologically resembling the DCT.

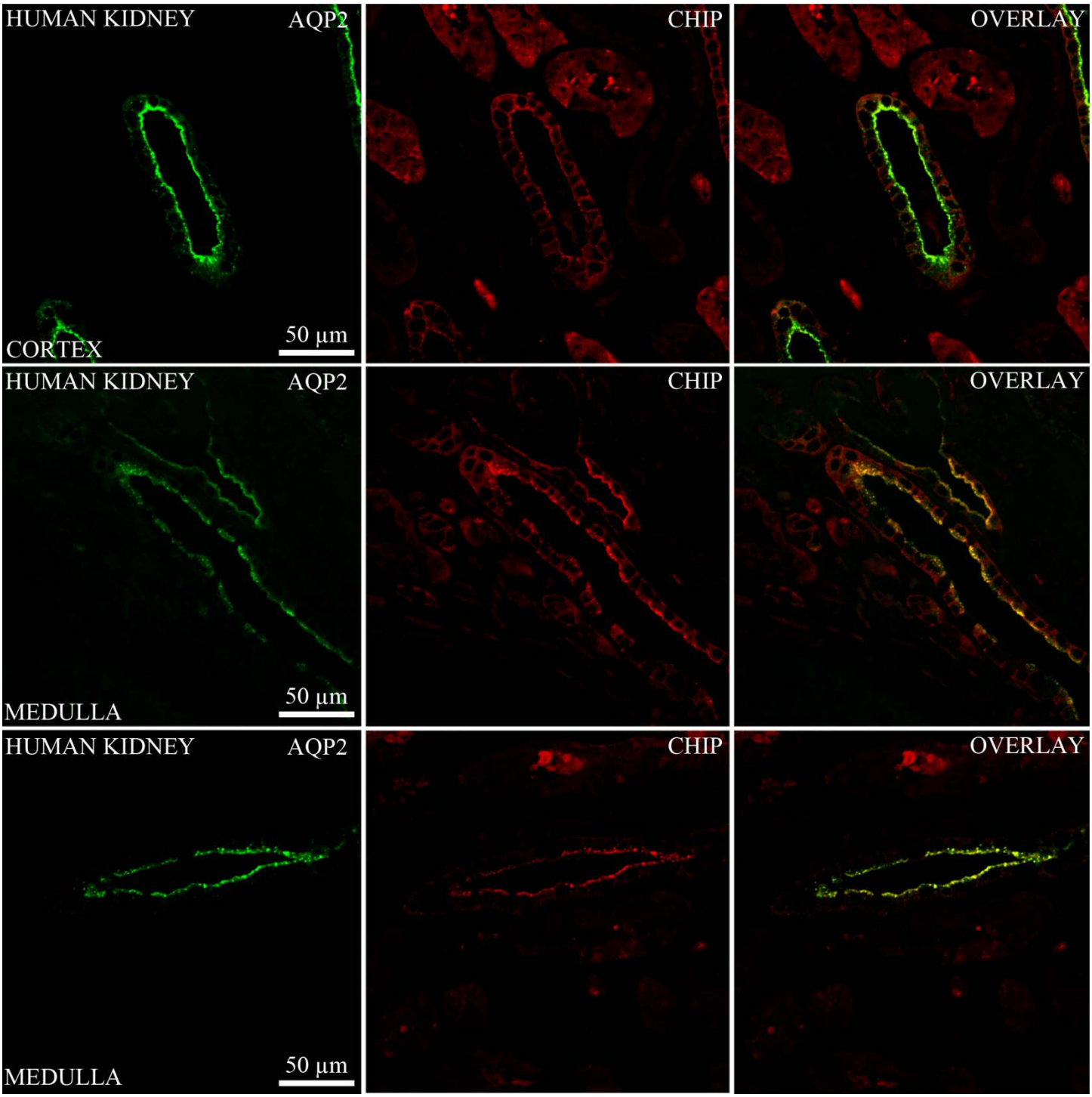

Supplemental Figure 11. Immunohistochemical localization of CHIP in human kidney. Confocal images of CHIP and AQP2 distribution in human kidney cortex and medulla. CHIP is expressed in collecting duct principal cells where it partially colocalizes with AQP2.

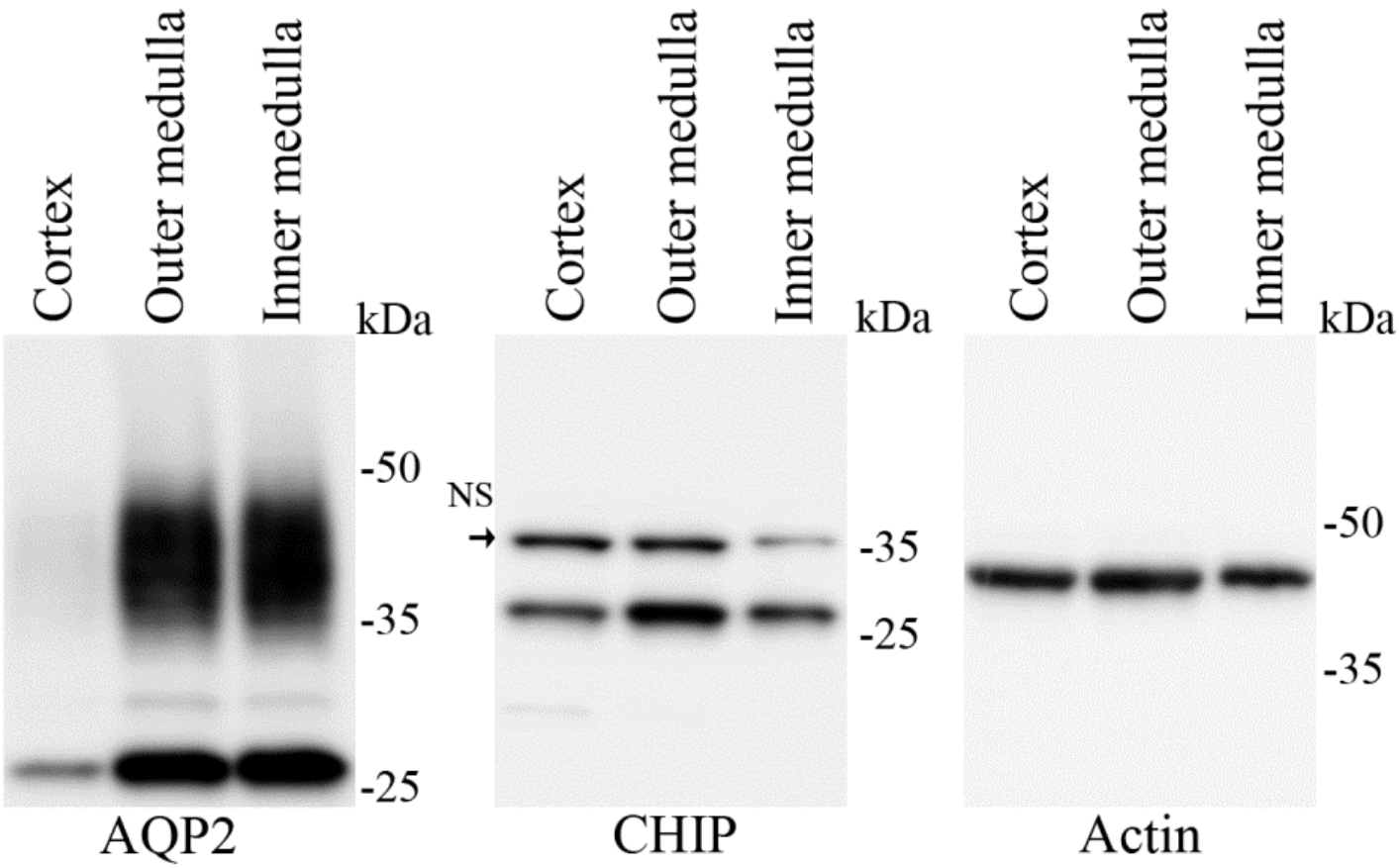

Supplemental Figure 12. CHIP distribution in different mouse kidney zones. Immunoblotting of total protein homogenates isolated from mouse kidney cortex, outer medulla and inner medulla demonstrate that CHIP is abundantly expressed in all regions examined. AQP2 is more abundant in the outer medulla and inner medulla. Immunoblotting for actin serves as a loading control.

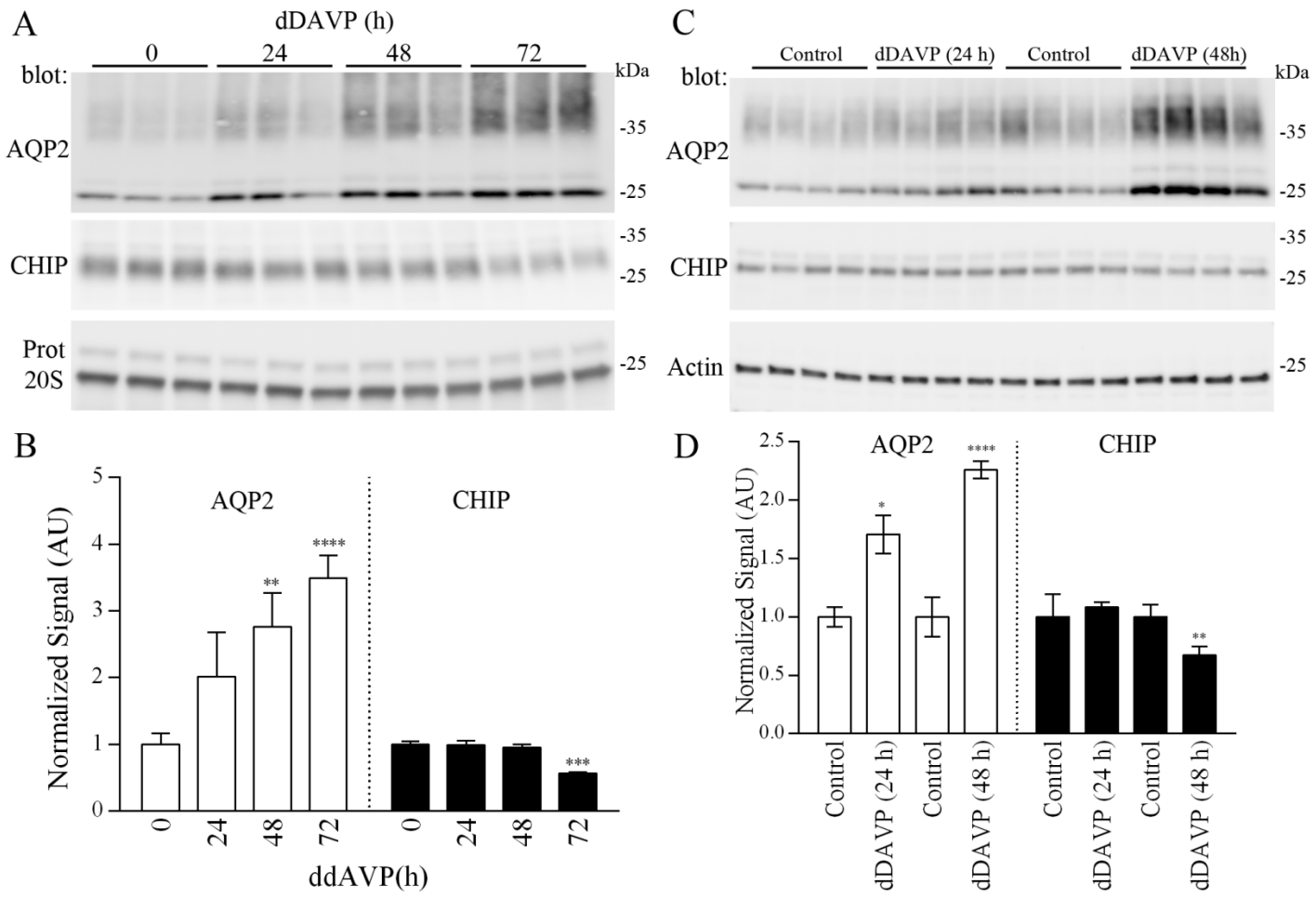

Supplemental Figure 13. *In vitro* and *in vivo* effects of dDAVP on CHIP and AQP2 abundance. A) Representative immunoblots of AQP2 and CHIP following dDAVP treatment of mpkCCD cells. B) Semi-quantitative summary of data. * indicates significance relative to 0 h time point. C) Representative immunoblots of AQP2 and CHIP in mice kidneys following dDAVP treatment of mice. Each lane represents an individual mouse sample. D) Semi-quantitative summary of data. * indicates significance relative to time-matched control group. *: 0.01<p<0.05; **: 0.001<p<0.01; ***: 0.0001<p<0.001; ****: p<0.0001.

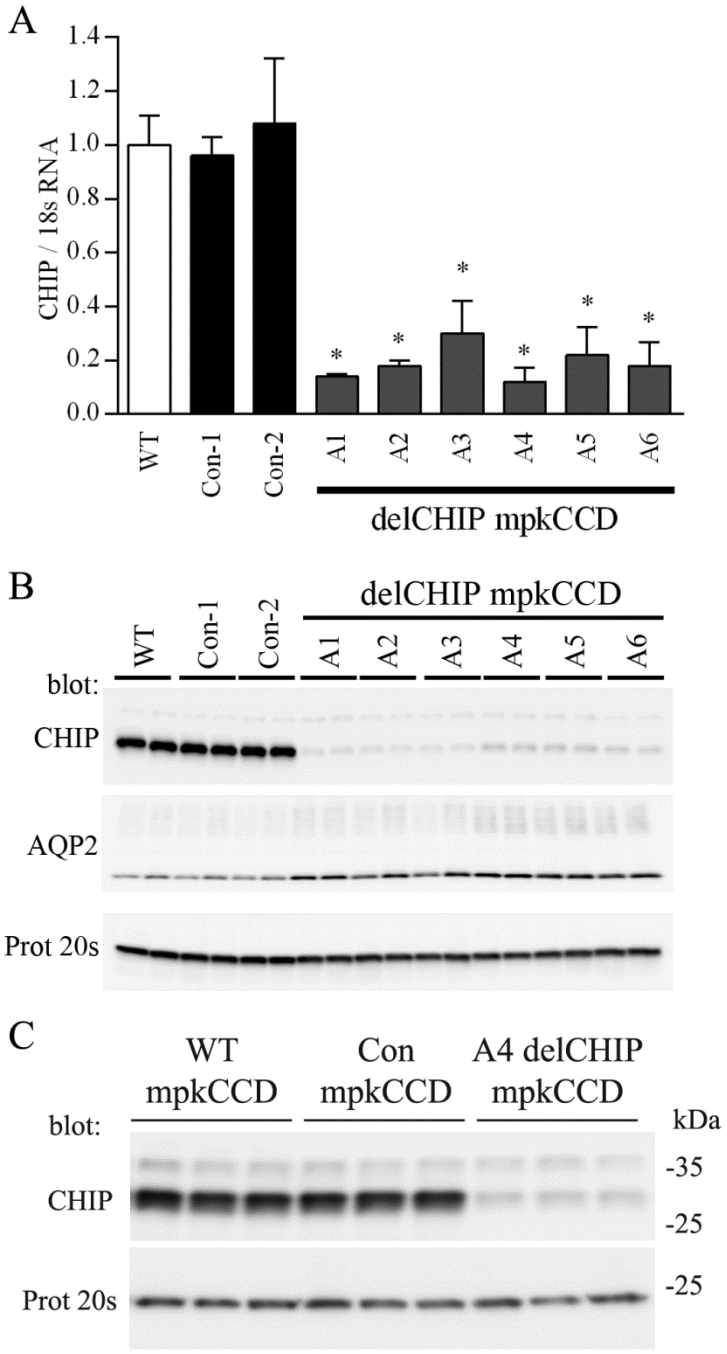

Supplemental Figure 14. Initial characterization of CHIP knockdown mpkCCD cells. A) RT-qPCR detection of CHIP mRNA levels in various lentivirus transduced CHIP shRNA expressing mpkCCD cells (A1-A6 delCHIP). Significant reductions in CHIP mRNA levels are observed in all the individual delCHIP lines relative to wildtype (WT) mpkCCD cells or scrambled shRNA control cells. B) Immunoblotting of CHIP demonstrates a clear reduction of CHIP protein in the A1-A6 delCHIP lines relative to wildtype (WT) mpkCCD cells or scrambled shRNA control cells. In each line the decrease in CHIP correlates with increased levels of AQP2. C) The A4delCHIP cells were used for the remainder of studies and showed a consistent reduction in CHIP protein levels relative to WT or scrambled shRNA expressing Con mpkCCD cells.

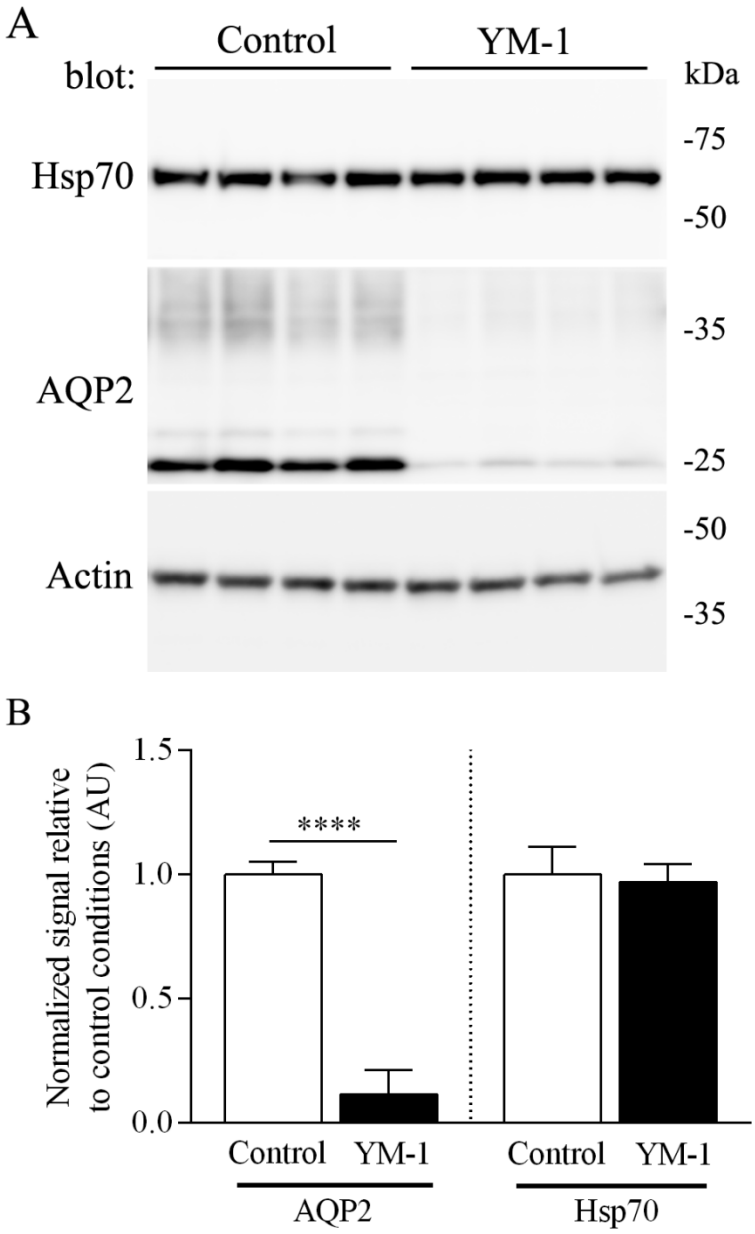

Supplemental Figure 15. Treatment of control mpkCCD cells with the Hsp70 activator YM-1 significantly reduces AQP2 levels. A) Immunoblotting of AQP2, Hsp70 and actin in samples isolated from cells treated with YM-1, which activates Hsp70 in a similar manner to Hip and stabilizes Hsp70 in its ADP-bound conformation favoring degradation of misfolded substrates. AQP2 levels are substantially reduced, strengthening the role of an Hsp70/CHIP dependent AQP2 degradation mechanism. Hsp70 levels are not affected by YM-1 treatment. Actin serves as a loading control. B) Quantification of AQP2 and Hsp70 in control and YM-1 treated mpkCCD cells. Values are obtained from 3 independent experiments with n = 3–4 for each individual treatment. * denotes significance between control and YM-1 treated cells. ****: $p<0.0001$.

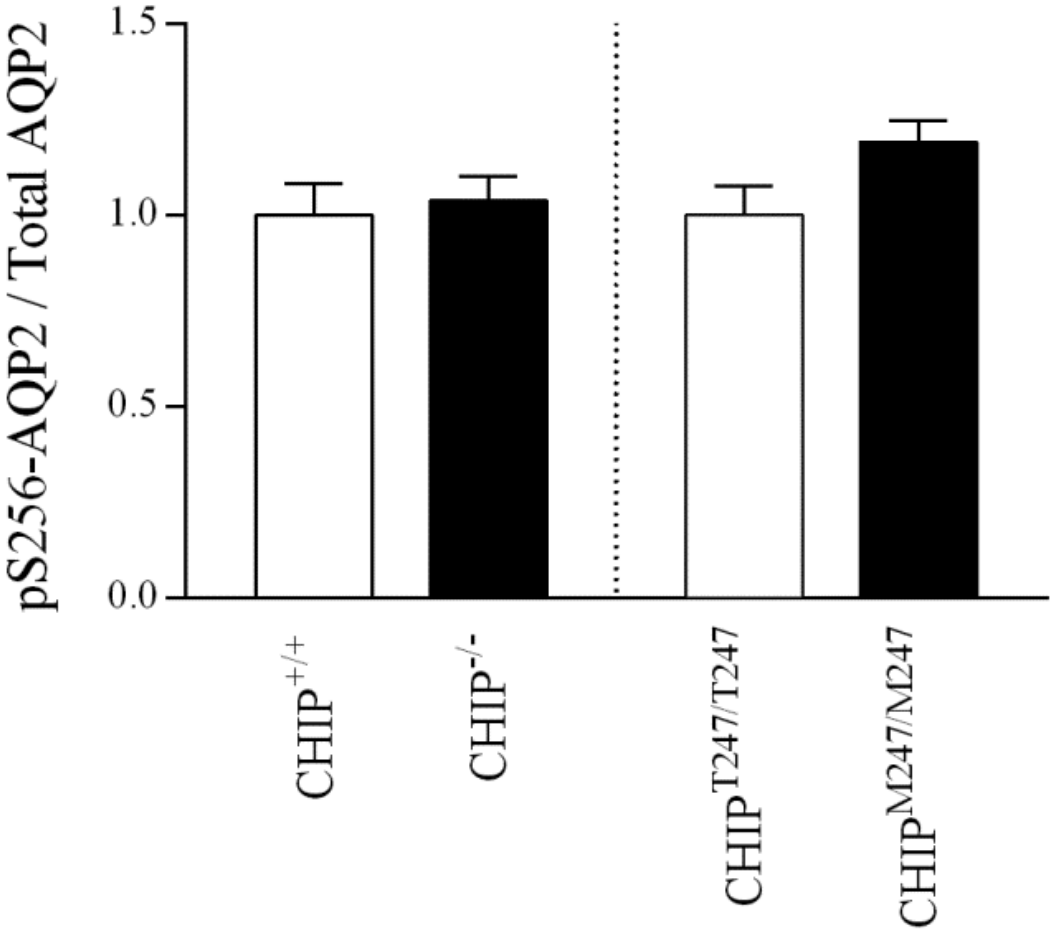

Supplemental Figure 16. pS256-AQP2 levels are not significantly greater in CHIP$^{-/-}$ and CHIP $^{M247/M247}$ mice when total AQP2 levels are considered. Summary of data from CHIP$^{+/+}$ mice and CHIP$^{-/-}$ mice (n=10/genotype) demonstrating that when normalized to total AQP2 the levels of pS256-AQP2 are not different between the genotypes. Similar results are observed for the CHIP$^{M247/M247}$ and CHIP$^{T247/T247}$ mice (n=6/genotype).

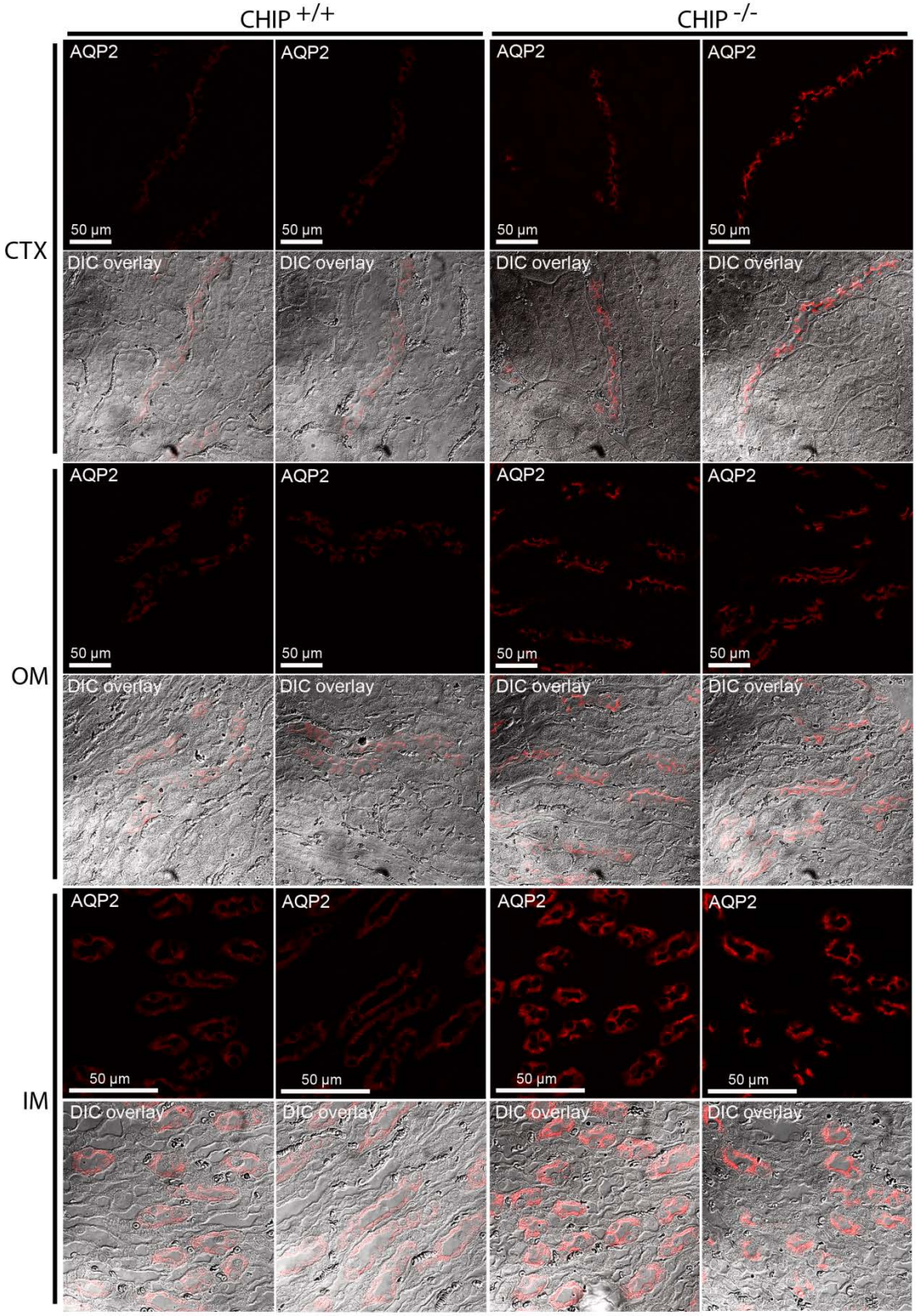

Supplemental Figure 17. Immunolabelling of AQP2 in kidneys from CHIP$^{+/+}$ and CHIP$^{-/-}$ mice. Images are representative confocal images of AQP2 expression in kidney sections from the kidney cortex, outer medulla and inner medulla of CHIP$^{+/+}$ and CHIP$^{-/-}$ mice. AQP2 levels were increased throughout the collecting duct in CHIP$^{-/-}$ mice, with apical labeling being more apparent. Differential interference contrast (DIC) images are provided to demonstrate the structure of the imaged section. A Leica TCS SL confocal microscope with an HCX PL APO 63× oil objective lens (numerical aperture: 1.40) was used with identical microscope settings (PMT offset and gain, sampling period, and averaging) for obtaining images. The dynamic range of the image acquisition was set so that the sections with the most intense fluorescence signal only had a few saturated pixels.

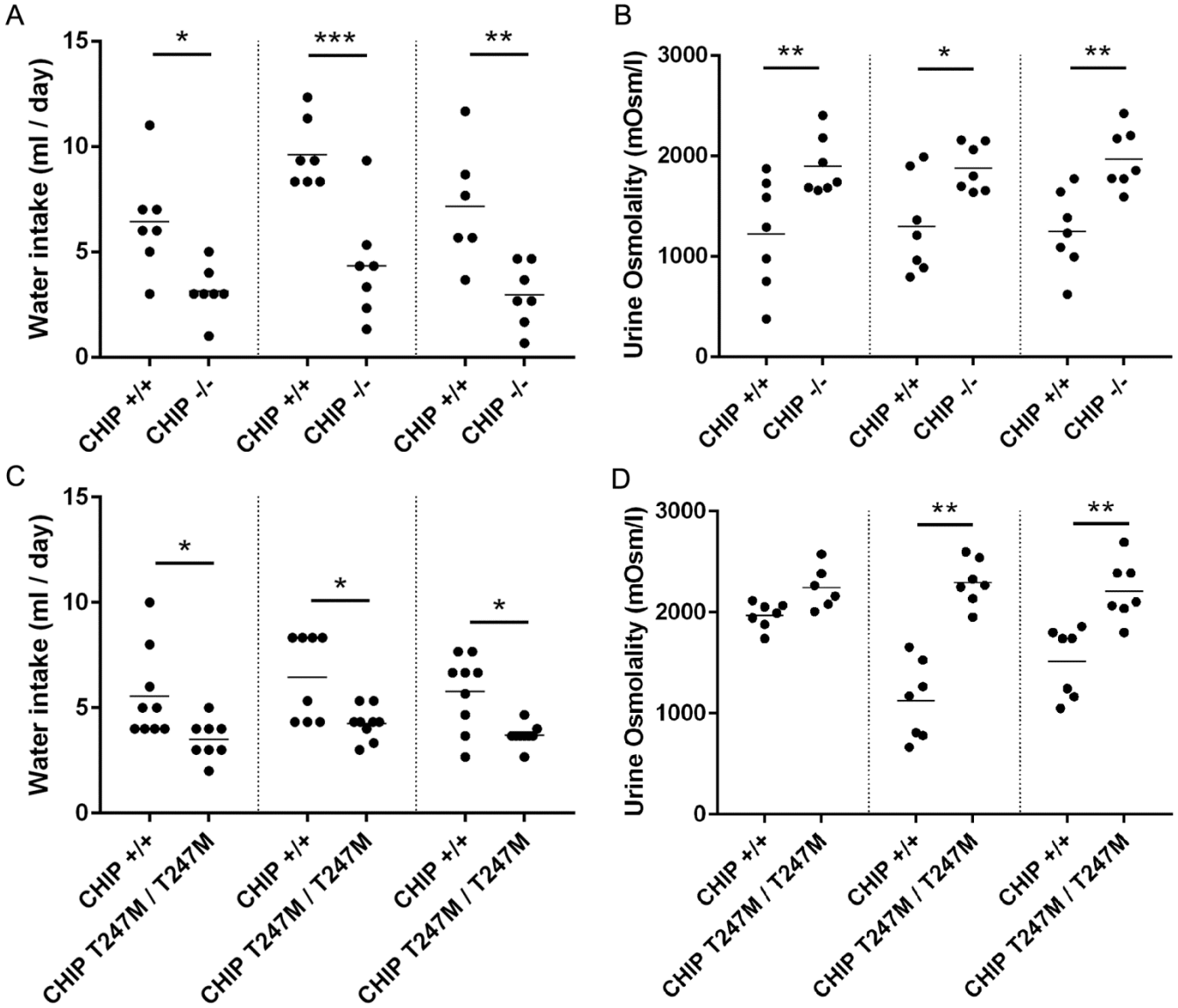

Supplemental Figure 18. Baseline renal water handling of CHIP$^{-/-}$ and CHIP$^{M247/M247}$ mice. A) CHIP$^{-/-}$ mice had decreased fluid intake on three successive days. B) The osmolality of spontaneously voided urine from CHIP$^{-/-}$ mice was significantly higher on each recorded day. C) CHIP$^{M247/M247}$ mice had decreased fluid intake on three successive days. D) The osmolality of spontaneously voided urine from CHIP$^{M247/M247}$ mice was significantly higher on the last two recorded days. * denotes significance between CHIP$^{+/+}$ and CHIP$^{-/-}$ or CHIP$^{T247M/T247M}$ mice. *: 0.01<p<0.05; **: 0.001<p<0.01; ***: 0.0001<p<0.001.

Supplemental Detailed Methods

Cell culture and SILAC labeling. mpkDCT and mpkCCD cells were grown at 37^{o}C/5%CO_2 in SILAC advanced DMEM/F12-Flex media (Invitrogen) containing 60 nM sodium selenite, 5 µg/ml transferrin, 2 mM glutamine, 50 nM dexamethasone, 1 nM triiodothyronine, 10 ng/ml epidermal growth factor, 5 µg/ml insulin, 20 mM D-glucose and 20 mM HEPES (pH 7.4) in light (mpkCCD; contains ^{12}C6 lysine, ^{12}C6 ^{14}N4 arginine, for mpkCCD) or heavy (mpkDCT; contains ^{13}C6 lysine, ^{13}C6 ^{15}N4 arginine, for mpkDCT) conditions for at least 5 passages to allow >97% labeling efficiency as confirmed by MS analysis. For experiments, cells were grown on semi-permeable supports (Transwell, Corning) until polarized monolayers were formed (transepithelial resistance (TER) >5 kΩ.cm^2). Cells were subsequently cultured in serum-free media (media changed every 12 h) in the following groups; 1) Control, 2) 1 nM [deamino-Cys1,D-Arg8]vasopressin (dDAVP) (10−9 M, Sigma) to only the basolateral side; 3) 1nM AngII (Sigma). After 4 days, cells were washed twice in ice-cold PBS and scraped in cell lysis buffer (8 M urea, 2 M thiourea, 50 mM Tris, pH 7.5) containing protease and phosphatase inhibitors (Halt protease and phosphatase inhibitors, Pierce). After 20 min incubation, lysates were sonicated on ice and centrifuged at 16,000g for 10 min at 4^{o}C. Supernatant protein concentration was measured by Bradford assay (Biorad), and equal protein amounts from mpkDCT and mpkCCD samples within each treatment group were pooled together. Per condition, four independent passages of cells were compared. Pooled samples were reduced, alkylated, and digested with trypsin and subjected to further high-pH reversed phase fractionation [1].

High-pH reversed phase fractionation. Peptides were loaded onto a ZORBAX Extend-C18 reversed phase column (Agilent, 3.5µm particle size, 4.6 x 150mm) and fractionated using Ultimate 3000 Liquid Chromatography (LC) (Dionex). Buffer A was 25mM NH_4FA in 100% H_2O

(pH adjusted to 9.5 with $NH_3 \cdot H_2O$) and buffer B was 25mM NH_4FA in 10% H_2O/90%ACN (equal volume of $NH_3 \cdot H_2O$ added as in buffer A). The fractionation was done by a linear gradient of 2-35% buffer B for 56 min plus a linear gradient of 35-80% buffer B for 8 min. One fraction was collected every 2 minutes, so there were 32 fractions in total. These 32 initial fractions were then combined into 8 final fractions through combining 4 fractions with the same time interval into one e.g. fractions 1, 9, 17 and 25 were pooled into final fraction 1. The final fractions were vacuum-dried and stored in -20°C until MS analysis.

Nano-liquid chromatography and mass spectrometry (nLC-MS) analysis. Fractionated peptides were analyzed by nano Liquid-Chromatography (nLC) (Easy LC 1000, Thermo Scientific) coupled to a Q-Exactive mass spectrometer (Thermo Scientific) through an EASY-Spray nano-electrospray ion source (Thermo Scientific). A pre-column (Acclaim®PepMap 100, 75 µm x 2 cm, C18, 3 µm, 100 Å, Thermo Scientific) was used to trap peptides and an analytical column (EASY-Spray Column, PepMap, 75 µm x 15 cm, C18, 3 µm, 100 Å, Thermo Scientific) was used to separate peptides. Buffer A was 100%H_2O/0.1% FA and buffer B was 100% ACN/0.1% FA. A 36-minutes linear gradient from 5% to 35% buffer B was used to separate peptides. MS settings were as follows: full scans (m/z 300-1800) were performed at a resolution of 70,000 with an automatic gain control (AGC) threshold of 3e6, a maximum injection time (IT) of 100ms, and 12 data dependent MS/MS scans at a resolution of 17,500 with AGC of 1e5 and IT of 50ms. HCD collision energy was 28%. Dynamic exclusion was set at 30 s, and precursor ions with charge state unknown, +1 and above +8 were excluded for fragmentation.

MS data analysis. Identification and quantification were done by MaxQuant (version 1.5.2.8). Raw files from each biological replicate under each treatment condition were searched together

to generate a combined result. Data were searched against RefSeq mouse database (58513 sequences, downloaded Oct. 2014) plus normal contaminants. Multiplicity was set to 2, with Arg10 and Lys6 as heavy labels. Acetylation of Protein N-term, oxidation of methionine, and phosphorylation of serine, threonine and tyrosine were set as variable modifications, and they were also included in protein quantification. iBAQ calculation was turned on. All other parameters, including precursor and fragment mass tolerances, were set as default values of MaxQuant. Proteins that were identified and quantified in at least three biological replicates were regarded as quantifiable proteins and subjected to Benjamini-Hochberg (BH) FDR estimations, and up-regulated proteins in one cell type (mpkDCT or mpkCCD) that passed 1% BH-FDR threshold were regarded as enriched proteins in that cell type. Proteins that had valid iBAQ values in one labeling channel (heavy or light) in at least three biological replicates and "zero" iBAQ values in the other channel in all replicates were regarded as unique proteins in either mpkDCT (heavy channel) or mpkCCD (light channel). The enriched plus unique proteins for each cell type (mpkDCT or mpkCCD) were defined as "specific" proteins for that cell type and retained for further analysis.

The Database for Annotation, Visualization and Integrated Discovery (DAVID) analysis. mpkDCT and mpkCCD specific proteins were subjected to DAVID (v6.7) functional annotation analysis. mpkDCT and mpkCCD specific protein accessions were transformed to gene symbols using Automated Bioinformatics Extractor (ABE) [2] and used as separate inputs. A customized background, containing all the protein accessions identified in this study, was used instead of the default *Mus musculus* background. In order for the DAVID to recognize as many background accessions as possible, the original RefSeq protein accessions were transformed to UniProt accessions using the ID Mapping tool from UniProt (http://www.uniprot.org/uploadlists/). Functional annotation clustering with default settings was performed separately on mpkDCT and

mpkCCD specific proteins against the customized background. Annotation clusters between mpkDCT and mpkCCD that share 50% or above individual annotations were mapped together and deemed identical, and a cluster name was given for each mapped cluster. Mapped clusters that had enrichment *p*-values no greater than 0.1 (corresponding to enrichment score no smaller than 1) in either mpkDCT or mpkCCD were retained to generate a heatmap, to illustrate which functions are more enriched in one cell type compared to the other.

Isolation of Enhanced Green Fluorescent Protein (EGFP) expressing mouse DCT cells. All animal protocols were performed in accordance to licenses for the use of experimental animals issued by the Danish Ministry of Justice. Mice had free access to standard rodent chow and water. Transgenic mice expressing EGFP driven by the parvalbumin promoter [3] were euthanized by cervical dislocation and kidneys quickly removed. The kidneys were sliced into approximately 1 mm pieces and incubated for 40 min in buffer B (125 mM NaCl, 0.4 mM KH2PO4, 1.6 mM K2HPO4, 1 mM MgSO4, 10 mM Na-acetate, 1 mM α-ketogluterate, 1.3 mM Ca-gluconate, 5 mM glycine, 30 mM glucose and 5 µg/mL DNase I (Sigma), pH 7.4) containing 2 mg/ml collagenase B (Roche). Samples were mixed continuously at 850 rpm at 37°C. After 10 min, half of the enzyme solution was removed and replaced with buffer B without collagenase, and samples were incubated for a further 10 min. This procedure was repeated for another 10 min. After a total incubation of 40 min, the tubular suspensions were passed through a 100 µM cell strainer (BD Falcon), and centrifuged for 3 min at 200 g. Cells were washed with a trypsin/EDTA solution (Lonza) containing 10 mM HEPES, 30 mM glucose and 50 ug/ml DNase I. Cells were again resuspended in trypsin/EDTA solution and incubated for 15 min at 37°C. Cells were washed in DMEM/HamF12 cell culture medium (Gibco) containing 5% FBS, 30 mM glucose, 10 mM HEPES and 50 mg/ml DNase I and subsequently resuspended in 1.5 ml medium. Cells were passed through a 40 µM cell strainer and kept at 4^0C. EGFP-positive and

negative cells were isolated on a FACSAria III (BD Biosciences) machine at the FACS Core Facility, Aarhus University, Denmark. Sorted cells were centrifuged for 10 min at 3,000 g at 4^0C and the pellet was resuspended in 1x Laemmli sample buffer (62.5 mM Tris, 8.75% Glycerol, 3% SDS, 89.5 µM Bromphenolblue, 15 mg/ml DTT, pH 6.8). Samples were heated for 10 min at 65^0C. EGFP purity changed from 4% before sorting to 94% after sorting in the EGFP-positive sample and 0% in the EGFP negative sample.

Antibodies. For western blotting, the antibodies utilized, the supplier and the predicted molecular weight of the target protein are detailed in Supplemental Table 7. Specificity of the commercial antibodies was based on that they either gave a single unique band on an immunoblot corresponding to the target proteins predicted molecular weight, or the most prominent band on the immunoblot was at the target proteins predicted molecular weight (with no other bands of similar size). Other characterized antibodies were AQP2 9398 [4] and pS256-AQP2 [5].

Fluorescent immunohistochemistry and confocal microscopy analysis. Specimens of human tissue were obtained post-mortem from the pathology archives at Aarhus University Hospital (http://www.en.auh.dk/departments/cancer+and+inflammation+centre/department+of+histopathology/research). Studies on this tissue were performed after approval from the local ethical committee, Aarhus County, Denmark. Archived paraffin-embedded mouse kidney tissue was processed as previously described [6]. Tissue from the CHIP gene-manipulated mice was immersion fixed in 4% PFA in PBS for 24 h before being processed as previously described [6]. Sections were immunolabeled for confocal laser scanning microscopy as previously described [6]

using CSN6 (sc47965), USP32 (sc374465), CHIP (sc133066), FBXO2 (sc393873), AQP2 C17 (sc9882) and NCC (SPC402D, Stressmarq). A Leica TCS SL confocal microscope with an HCX PL APO 63 x oil objective lens (numerical aperture: 1.40) was used for imaging of labelled sections (Leica Microsystems). For qualitative assessment of AQP2 abundance, microscope settings (PMT offset and gain, sampling period, and averaging) were equal for obtaining images. The dynamic range of the image acquisition was set so that the sections with the most intense fluorescence signal only had a few saturated pixels. Brightness was digitally enhanced on presented images.

Generation of mpkCCD cells with stable CHIP knockdown. MISSION lentiviral transduction particles against CHIP (numbers 8527, 8528, 8530, 280520, 280575) and corresponding control particles (SHC002V) were from Sigma. mpkCCD14 cells were cultured as described[7] in 24-well plates until 95% confluent. Cells were treated with hexadimethrine bromide (8 µg/ml final concentration) for 15 min in pure media, before addition of lentiviral particles (multiplicity of infection = 1.5). Transduction was allowed to proceed for 24 h, after which media was switched to mpkCCD14 media containing 2 µg/ml of puromycin for selection. Multiple clonal cell lines were isolated and individually characterized by examination of cell morphology, high TEER when grown on semi-permeable supports, CHIP expression levels by western blotting and RT-qPCR.

Real time quantitative PCR (RT-qPCR). Total RNA was isolated using the Ambion Ribopure kit (Invitrogen), treated with DNase I (Invitrogen), and reverse transcribed using Superscript II and random primers (Invitrogen); all steps were performed according to the manufacturer's instructions. A control reaction without the reverse transcriptase enzyme was performed to

exclude genomic DNA amplification. Primer pairs utilized spanning an exon-exon junction or an intron were: AQP2 (5′-TGGCTGTCAATGCTCTCCAC and 5′-GGAGCAGCCGGTGAAATAGA); STUB (5'-TCTACCCTCAATTCCGCCTT and 5'-GTGGCAGCGGTCATTGAGAA); 18S RNA (5′-GGATCCATTGGAGGGCAAGT and 5′-ACGAGCTTTTTAACTGCAGCAA). Specificity of the amplified products was determined using melting curve-analysis software, gel electrophoresis, and sequencing. Amplification was performed using the cDNA equivalent of 5 ng of RNA, 5 pmol of each primer and either HotStar Taq polymerase (Qiagen) or SYBR Green I Master Taq (Roche Applied Science). Cycling conditions were: 95 °C for 5 min, followed by 40 cycles of 95 °C for 10 s, 60 °C for 20 s, and 72 °C for 30s. RT-qPCR reactions were run on a LightCycler 480 (Roche), with fluorescence measured at the end of each elongation step to calculate Ct values. Relative quantitation of gene expression was determined using the comparative Ct method. Signals for ribosomal 18S RNA amplified in parallel were used to normalize for differences in the amount of starting cDNA.

mpkCCD14 culture and experimental conditions for CHIP analysis. mpkCCD14 cells were cultured on semi-permeable supports (0.4 µM pore size, Corning) until a confluent monolayer formed and TER was above 5 kOhm/cm2. 1 nM dDAVP was added in serum-free media to the basolateral compartment for 72 h to induce AQP2 expression. For acute dDAVP stimulation, cells were washed twice in pure media and reincubated in pure media for 3 h before re-stimulated with dDAVP (1 nM) from the basolateral side for 20 min at 37 °C. In dDAVP washout experiments, cells were subsequently washed twice in pure media and reincubated for 30 min at 37 °C before sample preparation. For 17-N-allylamino-17-demethoxygeldanamycin (17-AAG) studies, where indicated cells were incubated with 2µM 17-AAG for 16h before harvest. For Hsp70 activation studies, where indicated cells were incubated with 5 µM 2-[[3-Ethyl-5-(3-methyl-2(3H)-benzothiazolylidene)-4-oxo-2-thiazolidinylidene]methyl]-1-methyl-pyridinium

chloride (YM-1, Sigma) for 16h in the presence of dDAVP before harvest. For proteasomal and lysosomal inhibition experiments, after 72 h of dDAVP treatment, cells were washed twice in pure media and re-incubated in pure media for 8 h in the presence of 10 μM lactacystin, 150μM chloroquine or both, as indicated. For studies examining the long-term effects of ddAVP, cells were incubated with 1 nM dDAVP from the basolateral side for indicate time points. For cycloheximide chase studies, cells were incubated for various time points at 37 °C and 5% CO2 in 50 μM cycloheximide. Cells were washed twice in PBS and proteins were extracted in Laemmli sample buffer containing 10 mg/ml of DTT. For calculation of the protein half-life, average band densities for each time point were normalized to control and fitted using nonlinear regression and a one-phase exponential decay equation using GraphPad Prism software. Data were obtained from four independent experiments, with 3–6 observations for each individual time point.

Effects of dDAVP in mice. All animal work has been conducted according to relevant national and international guidelines. Animal housing conditions and experiments were approved by the Danish Ministry of Justice. Care of animals was in accordance with institutional guidelines. Mice were housed individually in metabolic cages and received 1 ng/h dDAVP via osmotic minipump for the indicated timeframes. Control animals received saline vehicle. At the end of the experiment, mice were euthanized by cervical dislocation and the kidneys processed as previously described [8].

Surface biotinylation of mpkCCD14 cells. Apical plasma membrane proteins were labeled with EZ-link hydrazide-biocytin (Pierce) as previously described [9].

Immunoblotting. Standard procedures were utilized for sample preparation and SDS-PAGE. Immunoblots were developed using ECL detection and signal intensity in specific bands were quantified using Image Studio Lite (Qiagen) densitometry analysis.

Immunoprecipitation (IP) using mpkCCD14 cells. IP was performed as previously described[4].

Mouse models of CHIP dysfunction. All animal use was approved by the Institutional Animal Care and Use Committee at the University of North Carolina at Chapel Hill. Mice lacking CHIP expression (*Stub1* targeted knockout, gene ID: 56424) B6;129-*Stub1*^{tm1Cpat}/Mmnc (RRID:MMRRC_037422-UNC) on a mixed background of 129S/SvEv and C57BL/6 were previously reported [10]. For this line, knockout mice are delineated (CHIP$^{-/-}$) and control animals are age and sex matched wildtype littermate controls (referred to as CHIP$^{+/+}$).

Generation of CHIP (Stub1 gene) T247M mutant mice. *Guide RNA Cloning*: Guide RNA protospacer (target) sequences were cloned into a T7 promoter vector in context with guide RNA structural elements, allowing T7-mediated *in vitro* transcription to produce the full guide RNA molecule. A guanine was added to the 5' end of protospacer sequences that do not have a native 5' guanine to allow T7 *in vitro* transcription initiation. T7 ligation mixtures were transformed into Stellar competent cells. Miniprep DNA was sequence-verified. *Guide RNA In Vitro Transcription.* Guide RNA plasmids were linearized with DraI, purified by silica column (Qiaquick) and used as template for T7 *in vitro* transcription using the NEB HiScribe T7 kit. Reactions were performed at 37°C overnight as recommended by the manufacturer using 1000 ng linear guide RNA plasmid. After addition of DNAse I for 30 min, guide RNAs were purified

using Qiagen RNEasy mini kit, eluted in 30 µl RNAse-free microinjection buffer (5 mM Tris-Cl pH7.5, 0.1 mM EDTA) and quantitated on a Nanodrop spectrophotometer. *Guide RNA Activity Test*: The Cas9/guide RNA target region was PCR amplified from wild-type C57BL/6 DNA using primers Stub1-ScF1 (5'-GGAGACAGGAGTTGCCCACACA-3') and Stub1-ScR1 (5'-CAGTTCAGAACCCATCAGCAGG-3'). PCR product was purified on a silica minicolumn and eluted in 10 mM Tris-Cl pH8.5. *In Vitro Cleavage Assay*: Guide RNAs were tested for activity in 1x NEB restriction buffer 3, 1 mg/ml BSA, 30 µg/ml Cas9 protein, 300 ng target DNA and 600 ng guide RNA in a 20 µl reaction volume. A control reaction was performed in parallel with all components except guide RNA. Reactions were incubated at 37°C for 1 hr followed by 80°C for 10 min, separated on 2% Agarose TAE gels and imaged using a standard ethidium bromide gel imaging system. Guide RNA Stub1-g82T (GAACCCTGCATTACACCCAGTGG, protospacer associated motif NGG underlined) produced nearly 100% target site cleavage. *Mouse production*: Genome editing was performed using CRISPR/Cas9 technology with the modification of mouse sequence NM_019719 at ntds #740 and #741 resulting in change of Threonine247 to Methionine (ACA to ATG). Founder animals were produced by microinjection of C57BL/6J embryos with a mixture of 100 ng/ul Cas9 mRNA, 50 ng/ul Stub1 guide RNA g82T and 100 ng/ul donor oligonucleotide Stub1-T247M-T (5'-TGACTACTTGTGTGGCAAGATTAGCTTTGAGCTGATGCGGGAACCCTGCATTATGCC CAGTGGTATCACCTATGACCGCAAGGACATTGAGGAGCACCTGCAGGTAAG-3') in 5 mM Tris pH7.5, 0.1 mM EDTA. Injected embryos were surgically implanted in CD-1 pseudopregnant recipients and resulting pups were genotyped by PCR amplification of the Stub1 T246 region followed by Sanger sequencing. Animals harboring the Stub1 T246M codon change were identified by deconvolution of sequence traces. Founder animals were mated to wild-type C57BL/6J animals and F1 animals harboring the T246M mutation were intercrossed to generate homozygous animals ((*Stub1* endonuclease-mediated mutation, gene ID: 56424) C57BL/6J-Stub1<em1Schiz> (MGI: 5883536)). For this line, knockin mice are delineated ($CHIP^{M247/M247}$)

and control animals are age and sex matched wildtype littermate controls (referred to as $CHIP^{T247/T247}$). *Off-target analysis*: For off-target analysis, guide RNAs were checked for predicted off-target sites using the web server crispr.mit.edu. The top 10 predicted off-target sites were PCR amplified from the founder biopsy DNA and PCR products were sequenced to detect the presence of mutations at each off-target site. Mutations were detected based on the presence of multiple peaks in the sequence traces.

CHIP gene modified mice kidney sample preparation. Kidneys were homogenized in ice-cold isolation solution (250 mM sucrose, 10 mM triethanolamine, pH 7.6, containing the protease inhibitors leupeptin (1 mg/ml) and Pefa-block (0.1 mg/ml) (Roche Applied Science) and phosphatase inhibitor mixture tablets (PhosSTOP, Roche Diagnostics A/S)) for generation of SDS-PAGE gel samples.

Water intake analysis and plasma and urine collection in CHIP mouse models. $CHIP^{-/-}$ or $CHIP^{M247/M247}$ and their respective wild-type controls were used to measure water intake and plasma and urine osmolalities. Animals were housed in individual cages on a 12/12 light/dark cycle with free access to standard rodent chow (Teklad) and water. We used $CHIP^{-/-}$ and $CHIP^{M247/M247}$ mice with their respective wild-type controls, balanced for sex and age (average age of 5.5 mo, range 3 mo - 9 mo, n = 7 - 8 mice per genotype). For daily water intake measurements, mice were moved to a procedure room isolated from outside interference to minimize accidental water loss. Three cages with no mice were manipulated in the same manner and used to control for water loss due to evaporation or spilling due to handling. The initial weight of the water bottles was measured and then at the same time for three consecutive days thereafter. Daily water intake was calculated assuming density of water = 1 g/ml.

Spontaneous urines were collected from the same cohort of mice towards the end of the light cycle on three consecutive days for a total of three collections per mouse. Mice were held individually above a piece of parafilm until spontaneous voiding occurred (usually within 1 min). Urine was transferred to a micro-centrifuge tube and frozen at -20^{o}C. Urine was centrifuged at 12,000 *g* for 10 min to remove precipitates before analysis. Mice were euthanized by way of carbon dioxide asphyxiation with a secondary method of vital organ collection. Blood plasma was prepared by collecting blood in BD Microtainer SST tubes (REF 365967). Urine and plasma osmolalities were measured using an Advanced Wide-Range Osmometer 3W2 (Advanced Instruments Inc., MA, USA). Sodium, potassium, chloride, urea and creatinine concentrations were measured in urine and plasma samples by the Clinical Pathology Laboratory at the Medical Research Council (Harwell, Oxfordshire, UK).

In vitro ubiquitylation reactions. Performed as previously described [11]. Briefly, 1 µM of bacterially-expressed Hsc70 was incubated in the presence of 2.5 µM CHIP, 1.6 µM of AQP2, 50 nM purified Ube1 (BostonBiochem, E305), 2.5 µM purified UbcH5c (BostonBiochem, E2-627) and 0.25 µM ubiquitin (BostonBiochem, U100H) in 50 mM Tris pH 7.5, 600 µM DTT, 2.5 mM $MgCl_2$-ATP (BostonBiochem, B20) in a total volume of 10 µl. Reactions were incubated for 1 h at 37 °C and stopped by 1:1 addition of 2X Laemmli sample buffer containing 5% β-mercaptoethanol and denatured at 100°C for 5 min. Samples were separated on a 4-15% Mini-PROTEAN® TGX Stain-Free™ Precast Gel at 150V and transferred to a PVDF membrane at 25V for 7 min using the Trans-Blot Turbo Transfer System (Bio-Rad). The membrane was blocked with 5% milk for 1 h at room temperature before immunoblotting with the appropriate primary antibodies: rabbit anti-AQP2 1:1,000 (H7661), rat anti-HSC70 1:5,000 (Enzo, ADI-SPA-815), mouse anti-CHIP 1:2,000 (Sigma, S1073) overnight at 4°C. Blots were then incubated for 1 h at room temperature with anti-mouse, anti-rabbit 1:10,000 (CST, 7076S and 7074S) or anti-

rat 1:10,000 (Sigma, A5795) IgG-HRP linked secondary antibodies and were developed using Clarity™ Western ECL Substrate (Bio-Rad) and imaged using the EC3TM Imaging System (UVP).

Statistics. For western blotting and mouse physiological recordings, data are expressed as mean±S.E.M. For two groups, data meeting the statistical assumptions of normality were assessed using an unpaired Student`s *t*-test. Comparisons of more than two groups were performed using either a one-way ANOVA or two-way repeated-measures ANOVA followed by Student-Newman-Keuls or Tukey's multiple comparison tests, respectively. Significance was considered at $P < 0.05$. The researchers were not completely blinded during sample collection and data acquisition/analysis.

REFERENCES

1. Yang F, Shen Y, Camp DG, 2nd, Smith RD: High-pH reversed-phase chromatography with fraction concatenation for 2D proteomic analysis. *Expert Rev Proteomics* 9: 129-134, 2012
2. Hoffert JD, Pisitkun T, Saeed F, Song JH, Chou CL, Knepper MA: Dynamics of the G protein-coupled vasopressin V2 receptor signaling network revealed by quantitative phosphoproteomics. *Mol Cell Proteomics* 11: M111 014613, 2012
3. Meyer AH, Katona I, Blatow M, Rozov A, Monyer H: In vivo labeling of parvalbumin-positive interneurons and analysis of electrical coupling in identified neurons. *J Neurosci* 22: 7055-7064, 2002
4. Moeller HB, Aroankins TS, Slengerik-Hansen J, Pisitkun T, Fenton RA: Phosphorylation and ubiquitylation are opposing processes that regulate endocytosis of the water channel aquaporin-2. *J Cell Sci* 127: 3174-3183, 2014
5. Hoffert JD, Fenton RA, Moeller HB, Simons B, Tchapyjnikov D, McDill BW, Yu MJ, Pisitkun T, Chen F, Knepper MA: Vasopressin-stimulated increase in phosphorylation at Ser269

potentiates plasma membrane retention of aquaporin-2. *J Biol Chem* 283: 24617-24627, 2008

6. Moeller HB, Knepper MA, Fenton RA: Serine 269 phosphorylated aquaporin-2 is targeted to the apical membrane of collecting duct principal cells. *Kidney Int* 75: 295-303, 2009
7. Yu MJ, Miller RL, Uawithya P, Rinschen MM, Khositseth S, Braucht DW, Chou CL, Pisitkun T, Nelson RD, Knepper MA: Systems-level analysis of cell-specific AQP2 gene expression in renal collecting duct. *Proc Natl Acad Sci U S A* 106: 2441-2446, 2009
8. Fenton RA, Brond L, Nielsen S, Praetorius J: Cellular and subcellular distribution of the type-2 vasopressin receptor in the kidney. *Am J Physiol Renal Physiol* 293: F748-760, 2007
9. Moeller HB, Slengerik-Hansen J, Aroankins T, Assentoft M, MacAulay N, Moestrup SK, Bhalla V, Fenton RA: Regulation of the Water Channel Aquaporin-2 via 14-3-3theta and -zeta. *J Biol Chem* 291: 2469-2484, 2016
10. Dai Q, Zhang C, Wu Y, McDonough H, Whaley RA, Godfrey V, Li HH, Madamanchi N, Xu W, Neckers L, Cyr D, Patterson C: CHIP activates HSF1 and confers protection against apoptosis and cellular stress. *EMBO J* 22: 5446-5458, 2003
11. Jiang J, Ballinger CA, Wu Y, Dai Q, Cyr DM, Hohfeld J, Patterson C: CHIP is a U-box-dependent E3 ubiquitin ligase: identification of Hsc70 as a target for ubiquitylation. *J Biol Chem* 276: 42938-42944, 2001